Wind-assisted ship propulsion feasibility study

Veronica VIGNA [a,1], Massimo FIGARI [a,2]
[a] *Università di Genova, Naval Architecture, Electric, Electronic and Telecommunication Engineering dpt. (DITEN) Via Montallegro 1, Genoa, 16145, Italy*

Abstract. The harvesting of wind energy and its transformation into a thrust force for the ship propulsion is the basics of Wind-Assisted Ship Propulsion (WASP). The concept has been gaining in popularity in the last years due to the expected benefits in emission reduction. To exploit the benefits, a proper integration between the conventional diesel engine-screw propeller propulsion plant and the WASP is mandatory. This paper aims to study the integration of the Flettner rotor technology with a conventional ship propulsion plant with controllable pitch propellers. The method allows to evaluate the engine-propeller working points and, eventually the total ship propulsive power, considering the influence of the rotor and the wind conditions. The total ship power is modelled on the amount of power required to spin the rotor, providing a way to compare hybrid propulsive solutions in terms of fuel consumption and CO_2 emissions. A 3000 ton Ro-Ro/Pax ferry has been selected as a case study. Results on the parametric analysis of rotor dimensions and wind conditions are presented. Assuming fixed wind conditions, the effect of the rotor at different ship speeds is shown.

Keywords. Wind-Assisted Ship Propulsion (WASP), Flettner Rotor, Energy efficiency, Fuel Consumption,

1. Introduction

The Fourth IMO GHG STUDY 2020 evaluated that the share of shipping in global anthropogenic emissions has increased from 2.76% in 2012 to 2.89% in 2018. The same study reported that Carbon Intensity, measured in EEOI, reduced between 2012 and 2018 for international shipping as a whole as well as for most ship types. However, the pace of carbon intensity reduction slowed from 2015, with average annual percentage changes ranging from 1 to 2%. The projection to 2050 indicated a 90-130% of 2008 emissions, far from meeting the UN emission reduction goals.

[1]Corresponding Author: veronica.vigna@edu.unige.it, orcid=0000-0002-4921-6430, linkedin=veronica-vigna-navarch
[2]massimo.figari@unige.it, orcid=0000-0003-0911-7259, linkedin=massimofigari

The increasing environmental concern worldwide is becoming a drive for innovation in shipping emission reduction technologies.

A research program has recently been started by the authors with the goal of studying greener technologies and solutions capable of improving the energy efficiency of ships.

One of the best options for retrofitting, as well as for new ships, is the adoption of renewable energy sources. This study addresses the Wind Assisted Ship Propulsion (WASP).

Multiple WASP technologies are proposed for ships such as traditional sails and wing sails, kite and Flettner rotors. This study focuses on the Flettener rotor due to the following reasons: it is considered simple to install, it has a light weight impact and it is easy to operate. Flettner rotors are rotating cylinders (usually spin by an electric motor) that generate aerodynamic lift and drag when immersed in a fluid stream; the working principle belongs to the so called Magnus effect [8].

Some literature exists on the rotor physics. In [3] the rotor aerodynamics has been analyzed by means of numerical simulations to create a tool for the preliminary design. The simulation results are used to develop a model for lift and drag coefficients. In [1] a series of experiments were conducted to better understand the influence of Reynolds number on rotors. The data showed that Reynolds number does not influence the power consumption of the rotor. An analytical function for rotor power consumption is proposed. The authors also suggest to take into proper consideration the rotor mechanical systems when computing the actual power consumption. The rotor's power consumption is also analysed in [5]. In [6] different wind assisted technologies (rotor, wingsail and DynaRig) are compared and the most significant fuel savings have been provided by the Flettner rotor, with an average value of 9%. The aim of this study is to propose a model able to address the rotor propulsive thrust and its influence on the engine-propeller working point. The proposed model includes a parametric model of the rotor as well as of the diesel propulsion system. The final goal is to evaluate the ship fuel consumption and the expected fuel savings. Section 2 outlines the model, including a brief explanation of the chosen reference frames. In Section 2.4 the influence of the rotor on propulsion is deeply investigated with a focus on forces (lift, drag and thrust in particular). Section 3 illustrates a case study and some numerical results. Finally the conclusions and final remarks can be found in Section 4.

2. Ship Propulsion Modelling

In this section the models of the rotor and of the propulsion system are discussed.

2.1. Reference Frames

The reference frames used in this paper are in accordance with [4]. The inertial $\underline{n}_i$ frame ($\mathcal{O}_\mathrm{n}$, $\underline{n}_1$, $\underline{n}_2$, $\underline{n}_3$) is the geographical reference system fixed to the Earth, where $\underline{n}_1$ points towards the North, $\underline{n}_2$ to the East and $\underline{n}_3$ towards the center of the Earth. The body-fixed base $\underline{b}_i$ (Ω_b, $\underline{b}_1$, $\underline{b}_2$, $\underline{b}_3$) is fixed to the hull with $\underline{b}_1$ pointing forward, $\underline{b}_2$ towards starboard and $\underline{b}_3$ downwards; the frame origin Ω_b is chosen to coincide with the center of the base of the rotor as reported in Figure 1, where Ψ [rad] is the Yaw angle and, for the purpose of this study, it is assumed equal to 0. The $\underline{f}_i$ base ($\mathcal{O}_\mathrm{f}$, $\underline{f}_1$, $\underline{f}_2$, $\underline{f}_3$): $\mathcal{O}_\mathrm{f} \equiv \Omega_\mathrm{b}$ is introduced to describe the wind related vectors: $\underline{f}_1$ is parallel to the apparent wind, as defined in section 2.3, and it has the same direction, $\underline{f}_2$ is perpendicular to the apparent wind and $\underline{f}_3$ is pointing downwards, as it can be seen in Figure 1, where α_f represents the angle between $\underline{b}_1$ and $\underline{f}_1$.

The transformations between the bases $\underline{b}_i$ and $\underline{f}_i$ are described by the following equations, where α_{app} is the angle between $\underline{b}_1$ and the direction of the incoming apparent wind:

$$\begin{cases} \underline{f}_1 = -\cos(\alpha_{app})\underline{b}_1 - \sin(\alpha_{app})\underline{b}_2 \\ \underline{f}_2 = \sin(\alpha_{app})\underline{b}_1 - \cos(\alpha_{app})\underline{b}_2 \\ \underline{f}_3 = \underline{b}_3 \end{cases}$$

2.2. *Methodology*

The proposed methodology integrates the Flettner rotor equations into the well-known engine-propeller matching procedure.
The methodology can be summarised by the following steps:

1. rotor forces and their influence on the ship forward motion.
2. effective net resistance ($\underline{R}_\mathrm{N}$) that the propeller have to balance, taking into account the presence of the rotor.
3. propeller working point by imposing the equilibrium between the propeller thrust and the ship net resistance ($\underline{T}_\mathrm{P} = \underline{R}_\mathrm{N}$) at a specific ship speed. The propeller speed $\mathrm{n_p}$ is calculated by using the $\mathrm{K_T}/\mathrm{J}^2$:

$$\frac{\mathrm{K_T}}{J^2} = \frac{\mathrm{R_N}}{\rho \cdot V_A^2 \cdot (1-t) \cdot D_p^2} \tag{1}$$

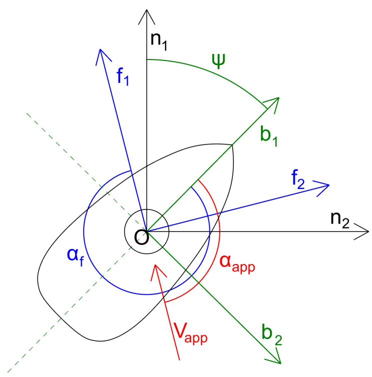

Figure 1. Reference frames.

where J is the propeller advance coefficient $V_A/(n_p \cdot D_p)$; ρ is the water density; $V_A = V \cdot (1-w)$; V is the ship speed, w the wake coefficient, t the thrust deduction factor, and D_p the propeller diameter.

4. required propeller-engine power to achieve the ship speed as:

$$P_B = \frac{P_O}{\eta_r \eta_s \eta_g} = \frac{2\pi\rho}{\eta_r \eta_s \eta_g} \cdot K_Q \cdot D^5 \cdot n_p^3 \qquad [W] \tag{2}$$

where P_O is the open-water propeller power, η_r is the rotative efficiency, η_s the shaft line efficiency and η_g the gear efficiency. Further details in [7].

5. power required to spin the rotor.
6. total ship propulsive power and KPIs.

2.3. Propeller thrust and net resistance

The propeller thrust is computed as the part of the ship resistance, i.e. net resistance, that is not overcome by the rotor forward force, as shown in Equation 3.

$$T_P \underline{b}_1 = R_N \underline{b}_1 \tag{3}$$

Equation (4) shows the different contributions to net resistance in terms of $\underline{b}_1$ components, where $\underline{R}_H$ is the hull resistance in calm condition (no air, no wind, no waves), $\underline{R}_W$ is the added resistance due to air friction on the whole ship (ship superstructure and rotor) and $\underline{T}_{FR}$ is the thrust generated by the rotor. It is important to underline that the net resistance also takes into account the added wind resistance due to the presence of the rotor as an appendix.

$$R_N \underline{b}_1 = R_H \underline{b}_1 + R_W \underline{b}_1 + T_{FR} \underline{b}_1 \tag{4}$$

2.4. Added Resistance and rotor forces

The air and wind added resistance includes the effect of the air friction and of the wind on the ship's superstructures (rotor included).

$R_W \underline{b}_1$ is determined as the effect of the wind on the transverse (S_T) ship projected area above waterline as reported by [2].

If the rotor is installed onboard but switched off, a further term to R_W must be added, considering the wind added resistance of the rotor as an additional superstructure.

On the contrary, when the rotor is working, there is no need for this additional term since the wind added resistance of the rotor will be incorporated in the subsequent aerodynamic considerations leading to the evaluation of $T_{FR} \underline{b}_1$.

Figure 2a can help in clarifying the explanation of the forces generated by the rotor.

$\underline{T}_{FR}$ is the effective thrust produced by the rotor in the ship direction; it is simply obtained as the projection along the ship longitudinal axis of the total force generated by the rotor ($\underline{F}$); the projection of $\underline{F}$ on the transverse axis is the

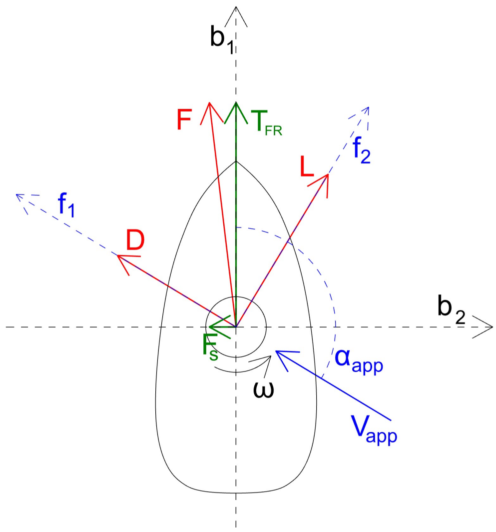

(a) Rotor forces.

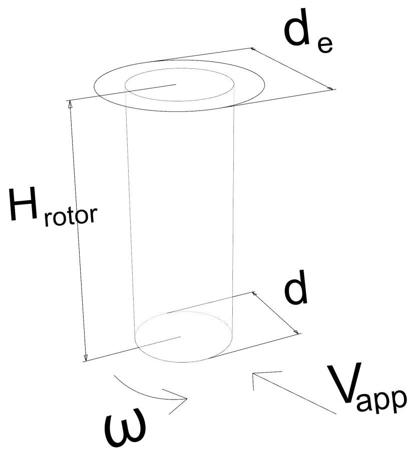

(b) Rotor geometry.

Figure 2. Rotor forces and geometry.

sway force $\underline{F}_S$.
The total force developed by the rotor $\underline{F}$ is the composition of rotor's aerodynamic lift ($\underline{L}$) and drag ($\underline{D}$): $\underline{F} = L\underline{f}_2 + D\underline{f}_1$.

The rotor lift and drag are computed using the lift (C_L) and drag (C_D) coefficients according to [3]. Lift and drag coefficient are related to the main rotor dimensions as shown in Figure 2b.

2.5. Power definitions and KPIs

The total ship propulsive power P_{TOT} is the sum of the engine mechanical power for the propeller and for the rotor, as reported in Equation (5).

$$P_{TOT} = \begin{cases} P_{TOT_{RotorOFF}} = n_{prop} \cdot P_{B_{Propeller@FRoff}} & \text{if Rotor is off} \\ P_{TOT_{RotorON}} = n_{prop} \cdot P_{B_{Propeller@FRon}} + n_{rotor} \cdot P_{B_{rotor}} & \text{if Rofor is on} \end{cases} \quad (5)$$

When the rotor is switched off P_{TOT} is simply the engine power P_B calculated for this configuration (with the resistance increased by $\underline{R}_W$), multiplied by the number of propellers. When the rotor is in use, the total propulsive power is the sum of P_B, calculated with the net resistance $\underline{R}_N$, multiplied by the number of propellers and the power required to spin the rotor $P_{B_{rotor}}$, times the number of rotors.

The mechanical power to spin the rotor $\mathrm{P_{absspin}}$ is evaluated as reported in [1], given that $U_{tan} = SR \cdot V_{app}$. In order to have homogeneous quantities, this power is converted in $\mathrm{P_{B_{rotor}}}$ the effective power required to spin the rotor considering the rotor transmission efficiency.

Key Performance Indicators (KPIs) are defined to monitor and eventually rank the analysed solutions. The first KPI is the Saved $P_{B_{propeller}}$, that can be defined as the difference between the propeller power required when the rotor is off with respect to the case when the rotor is on. This information is not sufficient to state whether the rotor is beneficial for the total power consumption of the ship or not; in fact the power required to spin the rotor is not included.

The second KPI adopted represents the percentage of power savings when the rotor is in use with respect when it is not available.

$$\text{Power savings gained using the rotor} = \frac{P_{TOT_{RotorOFF}} - P_{TOT_{RotorON}}}{P_{TOT_{RotorOFF}}} \cdot 100 \qquad (6)$$

This KPI is positive when the power required with the rotor in use is less than without it, so it is worth doing. On the contrary this KPI is negative when the rotor requires more energy than it can produce.

3. Case Study

A 3000 tons Ro-ro ferry with 2 CPP has been chosen as a case study. The ship speed and the wind conditions are consistent with a typical mainland-island connection service. The ship has been 'virtually' equipped with one Flettner rotor of variable geometric dimensions and it has been tested at different wind conditions. The rotor position considered in the calculations is located in the fore part of the ship, close to the fore mast, to maximize the wind effect. However, other aspects related to the rotor position such as structural aspects, visibility from the bridge, cargo operations in the fore part, etc. were not considered in this study.

The main ship characteristics and the initial values of the rotor dimensions are reported in Table 1.

Table 1. Main ship characteristics and initial values of the rotor dimensions.

Ship				Flettner rotor		
LOA	B	V_{cruise}	Power	H_{rotor}	d	SR
133 m	21.5 m	14 kn	3x3 MW	12.5 m	2.62 m	3

A parametric analysis of rotor forces $\underline{R}_W$ and $\underline{T}_{FR}$ have been performed. The effects of rotor dimensions, incoming wind direction and wind speed have been separately investigated.

3.1. Parametric Study of the Rotor Geometric Dimensions

Figure 3 shows the influence of rotor geometric dimensions on thrust. On the x-axis the operational ship speed is reported; on the y-axis the results are expressed in terms of rotor thrust over total ship resistance ratio ($\frac{T_{FR}}{R_H+R_W}$).
The wind condition is kept constant at 15 m/s and 110° direction. It can be noted that the distance between the curves tapers off as the ship speed increases, that means the effect of the rotor progressively reduces. This is mainly due to the ap-

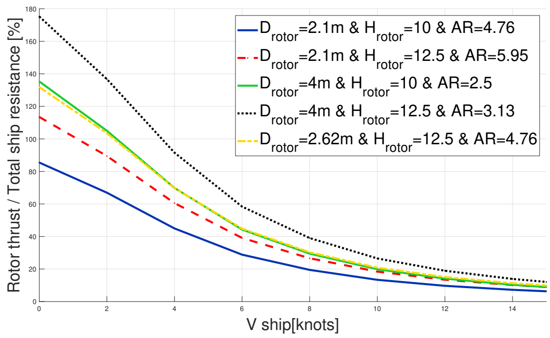

Figure 3. Influence of rotor's geometric dimensions on rotor thrust-ship resistance ratio $\frac{T_{FR}}{R_H+R_W}$

parent wind: at high speeds the apparent wind direction comes more from the bow, and thus the thrust generated decreases while the resistance increases. Another noticeable result is that forces increase with rotor size, in particular, enlarging the diameter is more effective than increasing its height (black dotted line). In [9] the analysis of wind and ship speed variations are extensively reported.

On the base of all the above mentioned parametric studies, a proper selection of the rotor dimension is achieved.

3.2. *KPI evaluation*

As defined in Section 2.5, the two KPI assumed are the Saved $P_{B_{propeller}}$ and the Total Power savings gained using the rotor. Figure 4a show the saved $P_{B_{propeller}}$ and the power absorbed to spin the rotor, respectively in blue and red colors. The ship speed is on the x-axis; the true wind is assumed constant (15 m/s from 100°). It is worth noting that savings increase with the ship speed. To confirm this result, also the power to spin the rotor $P_{B_{rotor}}$ must be addressed. $P_{B_{rotor}}$ is shown here with a red line and it is almost constant for each ship speed. This is because the power to spin the rotor is a function of the apparent wind speed, which, in this case, is not very much affected by the ship speed.

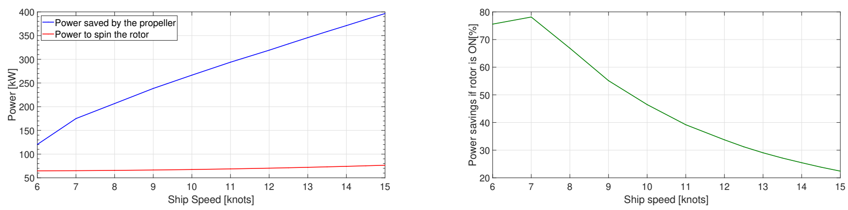

(a) Propeller power savings (b) Propulsive power savings percentage

Figure 4. Power savings.

The second KPI, namely, the percentage of total propulsive power savings, as shown in Equation (6), is shown in Figures 4b and 5.

Figure 4b presents the results of Equation (6) for various ship speed; it is computed for a specific wind condition of 15 m/s from 100°. The power savings reported are always positive and greater than 20%, thus, for this wind condition,

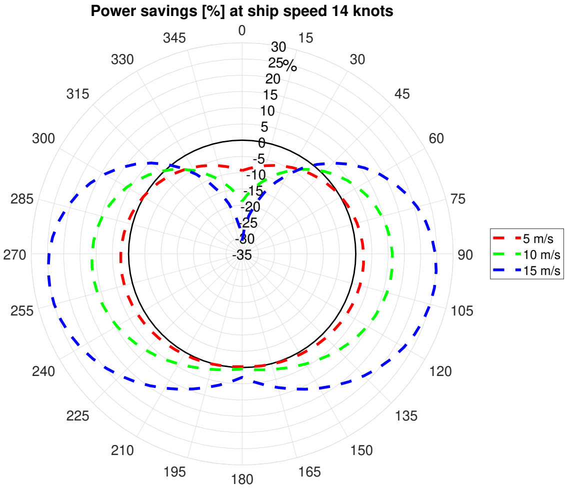

Figure 5. Power savings percentage when Rotor is on compared to when it is off.

the rotor is beneficial for every ship speed. In particular, at 10 knots of ship speed, the rotor is capable of ensuring more than 45% of power savings.

Figure 5 shows the second KPI, the percentage of power savings, for all true wind angles and for three true wind speeds (5 m/s in red, 10 m/s in green and 15 m/s in blue). The ship speed is kept constant at 14 knots. It is clear from Figure 5 that for a wind speed below 5 m/s, for this ship speed, the rotor should not operate, because it would lead to an additional power demand. In terms of direction of incoming wind, the best conditions are quarter winds and, the stronger the wind, the wider the range of suitable winds. For example, for a wind of 15 m/s from 100°, a power saving of more than 25% can be achieved.

4. Conclusions

Flettner rotor can play an important role in the ship propulsion plant decarbonization. The presented procedure is applied to a case study concerning a 3000 tons Ro-Ro/Pax ferry. It was found that the power requirements of the main engine can be reduced by 25% with favourable wind conditions. The parametric analysis of rotor dimensions showed a higher influence of rotor diameter and a lower importance of rotor high. For a more complete analysis of the rotor-propeller integration, not only power but also fuel consumption should be addressed. The next step of this study will be the estimation of the fuel consumption reduction achievable with the rotor.

References

[1] G. Bordogna, S. Muggiasca, S. Giappino, M. Belloli, J. A. Keuning, R. H.M. Huijsmans, and A. P. van 't Veer. Experiments on a flettner rotor at critical and supercritical reynolds numbers. *Journal of Wind Engineering and Industrial Aerodynamics*, 188, 2019.

[2] Jochim E. Brix. *Manoeuvering Technical Manual*. Seehafen Verlag GmbH, 1993.

[3] A. DeMarco, S. Mancini, C. Pensa, G. Calise, and F. DeLuca. Flettner rotor concept for marine applications: A systematic study. *International Journal of Rotating Machinery*, 2016, 2016.

[4] Thor I. Fossen. *Handbook of Marine Craft Hydrodynamics and Motion Control*. 2011.
[5] Akshay Lele and K. V.S. Rao. Net power generated by flettner rotor for different values of wind speed and ship speed. 2017.
[6] Ruihua Lu and Jonas W. Ringsberg. Ship energy performance study of three wind-assisted ship propulsion technologies including a parametric study of the flettner rotor technology. *Ships and Offshore Structures*, 15, 2020.
[7] M. Martelli and M. Figari. Real-time model-based design for codlag propulsion control strategies. *Ocean Engineering*, 141, 2017.
[8] Jost Seifert. A review of the magnus effect in aeronautics, 2012.
[9] V. Vigna, A. Coraddu, and M. Figari. Parametric study of the influence of the wind assisted propulsion on ships. In *MOSES 2021 - Proceedings of the 3rd international conference on modelling and optimisation of ship energy systems, MOSES2021 conference*, 2021.